The 2009 IEEE/RSJ International Conference on
Intelligent Robots and Systems
October 11-15, 2009 St. Louis, USA

Three–Dimensional Limit Cycle Walking with Joint Actuation

Kentaro Miyahara, Yuzuru Harada, Dragomir N. Nenchev and Daisuke Sato

Abstract— **This paper describes 3D biped walking generation and control based on Limit Cycle Walking. In our study, we use the simplest possible 3D biped model with three DOFs, incorporating roll and pitch motions in the frontal/sagittal planes, respectively. Our approach dynamically decouples these two motions, stabilizes pitch motion in the sagittal plane via the Limit Cycle Walking approach, introduces robustness for this motion using energy feedback control, and robustness for roll motion based on reference trajectory feedback tracking control. The roll reference trajectory is generated via analysis of the impact dynamics. Performance is verified via simulations.**

I. INTRODUCTION

In the near future, humanoid robots are expected to perform various tasks in our everyday life environment. Because of this perspective, research in the field has been advancing rapidly in recent years. At present, however, humanoid robots have just limited capabilities, such as biped walking, balance maintenance excluding external forces, simple communication and so on. Therefore, nowadays the field of application of humanoid robots is mainly education or entertainment. Further research is needed to broaden the capabilities of humanoid robots in the years ahead [1].

Central focus point in humanoid robot research is walking pattern generation and control. Most methods used so far have been based on the Zero-Moment-Point (ZMP) concept [2]. As an example, consider Kajita's Linear Inverted Pendulum Mode concept [3] which represents the dynamic model of a humanoid robot as an inverted pendulum that maintains the height of the center of mass (CoM). This method has found broad application because it ensures real–time performance and robust stability of walking by a simple mechanism.

ZMP–based methods have almost reached perfection. There are, however, two basic problems associated with such methods: energy efficiency and naturalness. We should note that ZMP–based methods make use of inverse kinematics to manipulate the ZMP or the CoM's position and velocity [4]. Therefore, singularities occurring at straight–knee configurations have to be avoided. Hence, it becomes impossible for the biped to take a stance with straight knees. This problem is related to energy efficiency because a bended–knee stance consumes more energy than a straight–knee one [5]. Several research works have already addressed in various ways the singularity/straight–knee problem under ZMP-based methods [6]–[8].

Another prospective method for walking pattern generation is the so-called Passive Dynamic Walk (PDW) method [9]. The underlying model is that of a simple passive biped walking down a slope, using thereby the gravity force in a natural way. A stable limit cycle is known to exist for PDW. The method can be regarded as the ultimate walking pattern generation method, from the viewpoints of energy efficiency and naturalness.

Recently, some research works appeared to address the extension of the PDW method to more realistic biped models, performing in 3D space. McGeer, for example, tried to model 3D PDW incorporating both roll and yaw rotation [10]. He found out that the walking pattern cannot be stabilized because of the dynamical roll–to–pitch or yaw–to–pitch coupling, inhibiting the generation of a stable limit cycle for pitch motion. Solutions for stabilizing the 3D walking pattern have been proposed by Kuo [11] and Wisse *et al.* [12], based on stabilizing roll motion and on using a pelvic body as yaw and roll compensator, respectively. As a result of these studies, one can conclude that decoupling plays an important role if one wishes to take advantage of the existing stable limit cycle of pitch motion.

There is a walking pattern generation method, called "Limit Cycle Walking," derived from the PDW concept. This walking method has been defined in [13] as "a nominally periodic sequence of steps that is stable as a whole, but not locally stable at any instant time." Note, however, that Limit Cycle Walking has some inherent problems, as follows:

- It is difficult to find a stable limit cycle.
- The generated walking motion is not robust, because there is no feedback component.
- The method is applied mostly to planar robots.

Because of these problems, Limit Cycle Walking based pattern generation is not suitable for direct practical application.

The aim of this work is addressing the problem of 3D walking pattern generation based on the Limit Cycle Walking concept. More specifically, we develop a method that decouples the dynamics in an appropriate way to take advantage of the existing stable limit cycle of pitch motion, in the sagittal plane only. Roll motion, on the other hand, is stabilized via ankle joint actuation. In addition, reconstruction of the gravity environment and energy feedback control for stabilizing pitch motion is applied. This combined control method ensures that pitch motion can be regarded as a planar robust dynamic walking based on the Limit Cycle Walking concept. The control method for roll motion is tracking control with specified reference trajectory. The reference trajectory is generated from analysis of the equation of collision.

The authors are with Musashi Institute of Technology, 1-28-1, Tamazutsumi, Setagaya-ku, Tokyo 158-8557, Japan
pdw@rls.mes.musashi-tech.ac.jp

978-1-4244-3804-4/09/$25.00 ©2009 IEEE

II. THE SIMPLEST THREE–DIMENSIONAL BIPED MODEL

This paper deals with the simplest 3D biped model as shown in Fig. 1. The model is composed of three links and three joints. The three links are the stance leg, the pelvis and the swing leg. The three joints are the ankle roll joint (Joint 1), the ankle pitch joint (Joint 2) and the hip pitch joint (Joint 3). Note that there is also a massless foot link. We assume the support leg to be always fixed to the ground. In this case, joint torques in the ankle joints can be applied relative to the massless foot link. The centroids of the three links are set at the midpoints. We assume that link inertia and joint friction can be ignored.

The generalized coordinates of the model are the joint angles: $\boldsymbol{q} = [\ q_1 \quad q_2 \quad q_3\ ]^T$, while the generalized force vector is represented in terms of joint torque as $\boldsymbol{\tau} = [\ \tau_1 \quad \tau_2 \quad \tau_3\ ]^T$. The total mass of the robot is defined as $m_t = m_1 + m_2 + m_3$.

Our biped is modeled as a hybrid dynamical system with two phases: the support phase, modeled with the equation of motion of a serial link chain, and the leg switch phase, modeled with the impact dynamics equation. It is assumed that leg switching occurs instantaneously.

A. Equation of motion

The equation of motion of the simplest 3D biped model during the support phase is given as:

$$\boldsymbol{M}(\boldsymbol{q})\ddot{\boldsymbol{q}} + \boldsymbol{C}(\boldsymbol{q}, \dot{\boldsymbol{q}})\dot{\boldsymbol{q}} + \boldsymbol{g}(\boldsymbol{q}) = \boldsymbol{\tau}, \tag{1}$$

where $\boldsymbol{M}(\boldsymbol{q}) \in \Re^{3\times3}$ denotes the inertia matrix $\boldsymbol{C}(\boldsymbol{q}, \dot{\boldsymbol{q}}) \in \Re^{3\times3}$ denotes the matrix for Coriolis and the centrifugal forces $\boldsymbol{g}(\boldsymbol{q}) \in \Re^3$ is the gravity term and $\boldsymbol{\tau} \in \Re^3$ is the control torque.

B. Equation of collision

The equation of collision models a collision between the swing leg's toe and the ground. We assume the collision is a completely inelastic one. Therefore the equation of collision is modeled after the principle of conservation of angular momentum:

$$\boldsymbol{Q}^+(\boldsymbol{q}^+)\dot{\boldsymbol{q}}^+ = \boldsymbol{Q}^-(\boldsymbol{q}^-)\dot{\boldsymbol{q}}^-, \tag{2}$$

where superscripts $(\circ)^-$ and $(\circ)^+$ denote pre– and post–collision values, respectively, $\boldsymbol{Q}^-(\boldsymbol{q}^-)\dot{\boldsymbol{q}}^-$ denoting the angular momentum at pre–collision and $\boldsymbol{Q}^+(\boldsymbol{q}^+)\dot{\boldsymbol{q}}^+$ that at post–collision, and the matrices $\boldsymbol{Q}^-(\boldsymbol{q}^-) \in \Re^{3\times3}$ and $\boldsymbol{Q}^+(\boldsymbol{q}^+) \in \Re^{3\times3}$ have the meaning of inertia matrices.

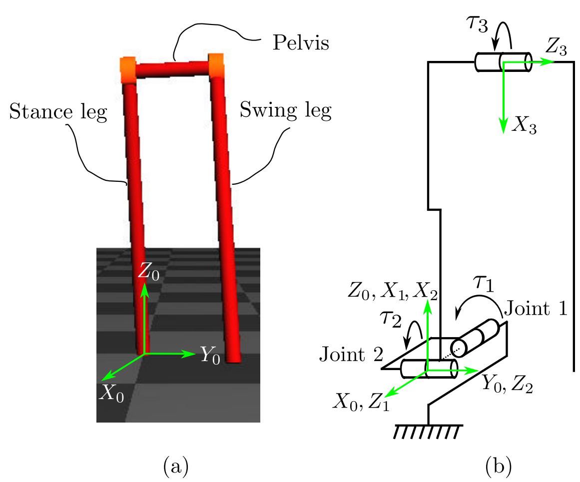

Fig. 1. The simplest 3D biped model: (a) rendered view, (b) kinematic structure with coordinate frames.

TABLE I

PHYSICAL PARAMETERS OF THE SIMPLEST 3D BIPED MODEL.

Link name	Length [m]	Mass [kg]
Stance leg	l_1 = 1.0	m_1 = 5.0
Pelvis	l_2 = 0.3	m_2 = 10.0
Swing leg	l_3 = 1.0	m_3 = 5.0

III. WALKING GENERATION AND CONTROL

Figure 2 shows the phase portrait of 3D PDW with slope angle $\phi = 0.02$ rad. As discussed in Section I, PDW in 3D is impossible because the roll motion cannot be energized by the gravity potential. Consequently there is no limit cycle.

To cope with the problem, we consider the design of a tracking control law for the ankle roll joint. However, roll motion with a reference trajectory has the following problems:

- Roll motion is coupled with pitch motion, therefore the limit cycle for pitch motion disappears.
- Roll motion must be synchronized with pitch motion within the existing limit cycle.
- The initial and the final values are unknown.

As a possible approach, we adopt decoupling control in combination with reconstruction of gravity environment plus energy feedback control for stabilizing pitch motion. This combined control method ensures that pitch motion can be regarded as planar robust dynamic walking based on the PDW concept. Thereby, we can deal with pitch motion as an independent planar motion.

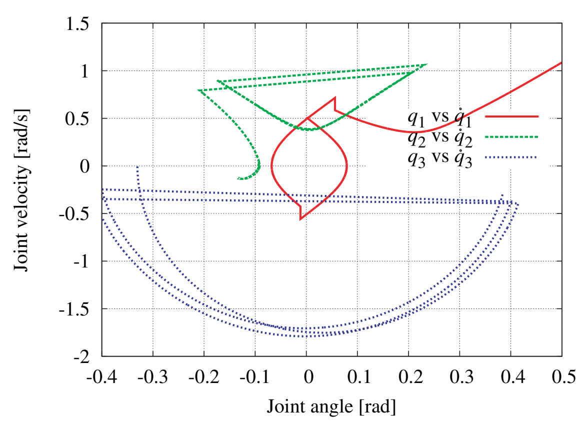

Fig. 2. Phase portrait of 3D Passive Dynamic Walking.

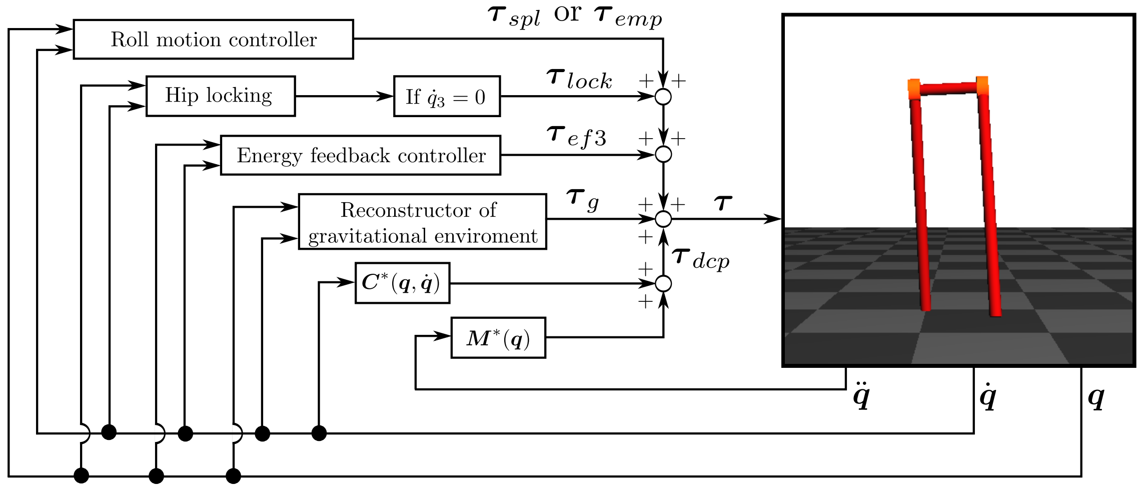

Fig. 3. Block chart of biped controller based on the decoupling control and the energy feedback control.

A. Control method for the pitch motion

1) Decoupling control: The decoupling control torque is calculated with the matrices $\boldsymbol{M}(\boldsymbol{q})$ and $\boldsymbol{C}(\boldsymbol{q}, \dot{\boldsymbol{q}})$ which are included in the equation of motion:

$$\boldsymbol{M}(\boldsymbol{q}) = \begin{bmatrix} M_{11} & M_{12} & M_{13} \\ M_{21} & M_{22} & M_{23} \\ M_{31} & M_{32} & M_{33} \end{bmatrix}, \tag{3}$$

$$\boldsymbol{C}(\boldsymbol{q}, \dot{\boldsymbol{q}}) = \begin{bmatrix} C_{11} & C_{12} & C_{13} \\ C_{21} & C_{22} & C_{23} \\ C_{31} & C_{32} & C_{33} \end{bmatrix}. \tag{4}$$

The second and the third rows of the equation of motion describe the moments on the two pitch joints (Joints 2 and 3). The first column of these two rows describes the coupling moment due to the roll joint (Joint 1). Consequently the coupling components of roll–to–pitch coupling are M_{21} M_{31} C_{21} and C_{31}. Therefore the matrices for decoupling control become:

$$\boldsymbol{M}^*(\boldsymbol{q}) = \begin{bmatrix} 0 & 0 & 0 \\ M_{21} & 0 & 0 \\ M_{31} & 0 & 0 \end{bmatrix}, \tag{5}$$

$$\boldsymbol{C}^*(\boldsymbol{q}, \dot{\boldsymbol{q}}) = \begin{bmatrix} 0 & 0 & 0 \\ C_{21} & 0 & 0 \\ C_{31} & 0 & 0 \end{bmatrix}. \tag{6}$$

With the help of these matrices the decoupling control torque becomes:

$$\boldsymbol{\tau}_{dcp} = \boldsymbol{M}^*(\boldsymbol{q})\ddot{\boldsymbol{q}} + \boldsymbol{C}^*(\boldsymbol{q}, \dot{\boldsymbol{q}})\dot{\boldsymbol{q}}. \tag{7}$$

This decoupling control torque is used as a feedforward control component.

2) Reconstruction of the gravity environment: We reconstruct the gravity environment for the pitch motion because the gravity environment is changed by the roll motion. The control torque which cancels the coupling between the roll motion and the pitch motion is calculated with the gravity term of the equation of motion $\boldsymbol{g}(\boldsymbol{q})$. This matrix in detail is expressed as:

$$\boldsymbol{g}(\boldsymbol{q}) = \begin{bmatrix} g_1 \\ g_2 \\ g_3 \end{bmatrix} = \begin{bmatrix} \alpha C_1 - \{\beta C_2 - \gamma S_{23}\} S_1 \\ (\gamma S_{23} - \beta S_2) C_1 \\ \gamma C_1 S_{23} \end{bmatrix} g, \tag{8}$$

where $S_1 = \sin q_1$ $C_1 = \cos q_1$ $S_2 = \sin q_2$ $C_2 = \cos q_2$ $S_{23} = \sin(q_2 + q_3)$ $\alpha = (m_2 + 2m_3) l_3/2$ $\beta = \{m_1 + (2m_2 + m_3)\} l_1/2$ $\gamma = m_3 l_2/2$. The components of roll–to–pitch coupling are the terms which include C_1 or S_1 in the second and the third rows. Consequently, the control torque for reconstruction of the gravity environment for the pitch motion becomes:

$$\boldsymbol{\tau}_g = \begin{bmatrix} g_1^* \\ g_2^* \\ g_3^* \end{bmatrix} = \begin{bmatrix} 0 \\ (\gamma S_{23} - \beta S_2)(C_1 - 1) \\ \gamma (C_1 - 1) S_{23} \end{bmatrix} g. \tag{9}$$

3) Energy feedback control: Energy feedback control was proposed by Asano *et al.* [14]. This control method stabilizes planar compass biped walking based on the PDW concept. It is known from the features of planar PDW that the rate of increase of the mechanical energy E w.r.t. the horizontal CoM position r_{Cx} is constant:

$$\frac{\partial E}{\partial r_{Cx}} = m_t g \tan \phi. \tag{10}$$

The time differential of this equation is:

$$\dot{E} = m_t g \dot{r}_{Cx} \tan \phi, \tag{11}$$

where $\dot{r}_{Cx}$ is the horizontal component of the CoM velocity vector. This equation expresses that the acceleration of the robot in the walking direction is concentrated at the CoM. Then, the desired energy trajectory E_d can be chosen as:

$$E_d(r_{Cx}) = m_t g r_{Cx} \tan \phi + E_0, \tag{12}$$

where E_0 is the desired energy value when $r_{Cx} = 0$ for steady motion. The following asymptotic stabilizing control has been proposed [14]:

$$\frac{d}{dt}(E - E_d(r_{Cx})) = -\zeta (E - E_d(r_{Cx})), \tag{13}$$

where ζ is a constant positive feedback gain. Using Eqs. (10) and (12), the time derivative of the energy error is:

$$\frac{d}{dt}(E - E_d(r_{Cx})) = \dot{\boldsymbol{q}}^T \boldsymbol{\tau}_p - m_t g \dot{r}_{Cx} \tan\phi, \tag{14}$$

where $\boldsymbol{\tau}_p = \begin{bmatrix} \tau_2 & \tau_3 \end{bmatrix}^T$ means the control torque for pitch motion. Therefore, based on Eqs. (13) and (14), we can solve the following indeterminate equation:

$$\dot{\boldsymbol{q}}^T \boldsymbol{\tau}_p = m_t g \dot{r}_{Cx} \tan\phi - \zeta(E - E_d(r_{Cx})). \tag{15}$$

As a solution, we choose the constant torque ratio condition:

$$\tau_2 = \mu\tau_3, \tag{16}$$

where μ is a constant. The solution of Eq. (15) with constant torque ratio is:

$$\boldsymbol{\tau}_{ef} = \begin{bmatrix} \mu \\ 1 \end{bmatrix} \frac{m_t g \dot{r}_{Cx} \tan\phi - \zeta(E - E_d(r_{Cx}))}{\mu\dot{q}_2 + \dot{q}_3}. \tag{17}$$

This control input is time–independent and maintains the property of autonomy. The energy feedback control torque for the simplest 3D biped model becomes:

$$\boldsymbol{\tau}_{ef3} = \begin{bmatrix} 0 \\ \boldsymbol{\tau}_{ef} \end{bmatrix}. \tag{18}$$

4) Synchronization between the pitch and the roll motion: The hip joint of the robot is locked at a specified timing for synchronization between the pitch and the roll motion. Specifically, we lock the joint when the velocity of the hip joint becomes zero: $\dot{q}_3 = 0$. The hip locking torque is derived from the Lagrange multiplier with constraint $\ddot{q}_3 = 0$:

$$\boldsymbol{\tau}_{lock} = \boldsymbol{J}^T \lambda, \tag{19}$$

where

$$\boldsymbol{J} = \begin{bmatrix} 0 & 0 & 1 \end{bmatrix}, \tag{20}$$

$$\lambda = -\{\boldsymbol{J}\{\boldsymbol{M}(\boldsymbol{q})\}^{-1}\boldsymbol{J}^T\}^{-1} \{\boldsymbol{J}\{\boldsymbol{M}(\boldsymbol{q})\}^{-1}(\boldsymbol{\tau} - \boldsymbol{C}(\boldsymbol{q}, \dot{\boldsymbol{q}})\dot{\boldsymbol{q}} - \boldsymbol{g}(\boldsymbol{q}))\}. \tag{21}$$

Because of the chosen lock timing, it is easy to synchronize the roll and the pitch motions.

B. Control method for roll motion

1) Control based on the analysis of the equation of collision: The first method is PD control of the ankle roll joint with a given reference trajectory which is generated by a spline function. The main point of this method is to determine the initial and the final values. As a method of determination we consider the equation of collision (Eq. (2)) and the known initial state of the robot $\boldsymbol{q}_{ini}$ $\dot{\boldsymbol{q}}_{ini}$. Here $\boldsymbol{q}_{ini}$ $\dot{\boldsymbol{q}}_{ini}$ coincide with $\boldsymbol{q}^+$ $\dot{\boldsymbol{q}}^+$. We determine the initial state of the robot as:

$$\boldsymbol{q}_{ini} = \boldsymbol{q}^+ = \begin{bmatrix} q_1^+ \\ q_2^+ \\ q_3^+ \end{bmatrix} = \begin{bmatrix} 0.0 \\ -0.19 \\ 0.38 \end{bmatrix} \text{rad}, \tag{22}$$

$$\dot{\boldsymbol{q}}_{ini} = \dot{\boldsymbol{q}}^+ = \begin{bmatrix} \dot{q}_1^+ \\ \dot{q}_2^+ \\ \dot{q}_3^+ \end{bmatrix} = \begin{bmatrix} -0.51 \\ -0.86 \\ 0.4 \end{bmatrix} \text{rad/s}. \tag{23}$$

The initial angle of the ankle roll joint is zero because we consider it acceptable that the robot posture is erect at the leg switching phase. In addition the initial velocity of the ankle roll joint is -0.51 rad/s which is an arbitrary value. Here, we adopt the same value as in the case of passive dynamic walking (see Fig. 2). The second and the third rows are the ankle and the hip pitch joints. The initial values are determined from planar dynamic walking with energy feedback control. The final joint angle of the robot $\boldsymbol{q}_{fin}$ can be calculated via $\boldsymbol{q}^+$:

$$\boldsymbol{q}_{fin} = \boldsymbol{q}^- = \begin{bmatrix} q_1^+ \\ q_2^+ + q_3^+ \\ -q_3^+ \end{bmatrix} = \begin{bmatrix} 0.0 \\ 0.19 \\ -0.38 \end{bmatrix} \text{rad}. \tag{24}$$

By substituting $\boldsymbol{q}_{ini}$ $\dot{\boldsymbol{q}}_{ini}$ and $\boldsymbol{q}_{fin}$ into the equation of collision (Eq. (2)) we can obtain the final state of the robot:

$$\dot{\boldsymbol{q}}_{fin} = \dot{\boldsymbol{q}}^- = \{\boldsymbol{Q}^-(\boldsymbol{q}^-)\}^{-1}\boldsymbol{Q}^+(\boldsymbol{q}^+)\dot{\boldsymbol{q}}^+ = \begin{bmatrix} -0.63 \\ 1.08 \\ 0.12 \end{bmatrix} \text{rad/s}. \tag{25}$$

In this way we can obtain the initial and the final states of the ankle roll joint angle which is the first component of $\boldsymbol{q}^\pm$ and the joint velocity which is the first component of $\dot{\boldsymbol{q}}^\pm$. The meaning of these components can be explained with the phase portrait shown in Fig. 4. The circular arc from I to II is the solution curve for the support phase of the right leg. The circular arc from III to IV is the solution curve for the support phase of the left leg. The jumps from II to III and from IV to I denote the leg switch phase. Here, $q_1^- = -0.63$ rad/s and $q_1^+ = -0.51$ rad/s stand for the state at the jump from IV to I. Consequently, a limit cycle can be generated when the same jump in the state occurs. The second and the third components in $\dot{\boldsymbol{q}}^-$ are identical with the final values of the ankle and the hip pitch joint velocity. Note, that the pitch motion is controlled by energy feedback control, thus stability is preserved. Therefore, we do not have to consider these values. Consequently, we can obtain the reference trajectory of the ankle roll joint which is calculated

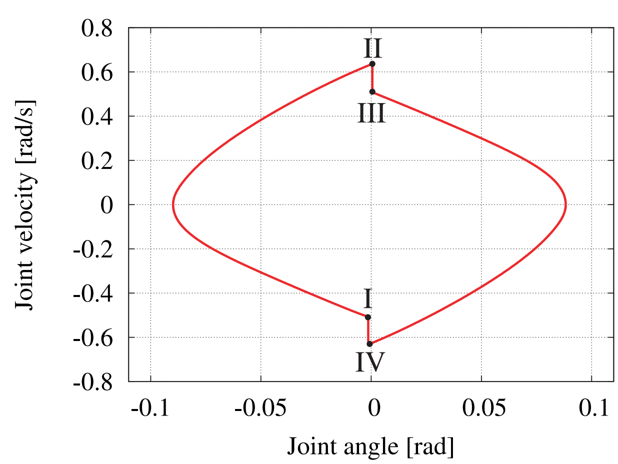

Fig. 4. Phase portrait of the ankle roll joint.

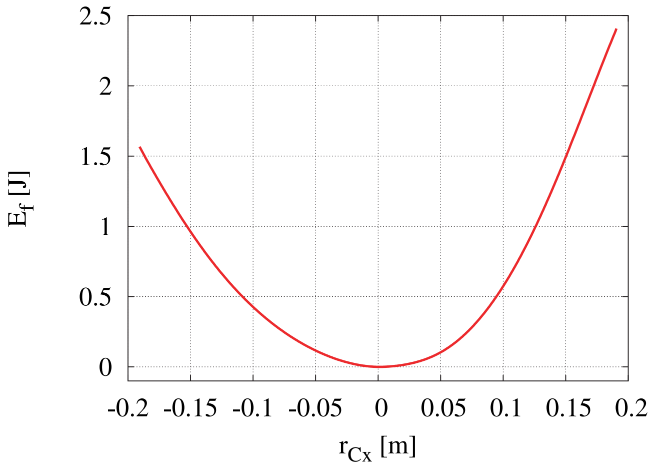

Fig. 5. Reference trajectory for energy feedback control of roll motion.

by the spline function. The reference trajectory for the ankle roll joint q_{1d} is:

$$q_{1d}(t) = a_0 + a_1 t + a_2 t^2 + a_3 t^3 + a_4 t^4 + a_5 t^5, \qquad (26)$$

where a_i, $i = 0, 1, ..., 5$ are the constant coefficients of the spline function, and t is the time. As constraint conditions, we choose: $q_{1d-0} = 0.0$ rad as the initial value of the ankle roll joint angle, $\dot{q}_{1d-0} = -0.51$ rad/s is the initial value of the ankle roll joint velocity, $\ddot{q}_{1d-0} = 0.0\ \mathrm{rad/s^2}$ as the initial value of the ankle roll joint acceleration, $q_{1d-f} = 0.0$ rad as the final value of the ankle roll joint angle, $\dot{q}_{1d-f} = 0.63$ rad/s as the final value of the ankle roll joint velocity, $\ddot{q}_{1d-f} = 0.0\ \mathrm{rad/s^2}$ as the final value of the ankle roll joint acceleration, and $t_f = 0.725$ s as the final time. Consequently, the first control method for the ankle roll joint becomes:

$$\boldsymbol{\tau}_{spl} = \begin{bmatrix} k_p(t)(q_{1d} - q_1) + k_d(t)(\dot{q}_{1d} - \dot{q}_1) \\ 0 \\ 0 \end{bmatrix}, \qquad (27)$$

where $k_p(t) = 1000t$ Nm/rad and $k_d(t) = 1000t$ Nms/rad are variable positive feedback gains used to avoid excessive joint torque during the leg switch phase. In addition time t is reset in the leg switch phase.

2) Empirical method: The second control method for the ankle roll joint is tracking control with an empirical reference trajectory based on the relation between the CoM position and the mechanical energy. The reason why we choose this relation is to imitate energy feedback control because the reference trajectory of energy feedback control is in fact a relation between the CoM position and the mechanical energy which includes the frontal plane velocity only. The reference trajectory is empirical therefore it is difficult to explain why we can obtain a trajectory for the relation between the CoM position r_{Cx} and the mechanical energy of the frontal plane $E_f = \frac{1}{2} m_t r_{Cy}^2$ which includes the frontal plane velocity r_{Cy} only. In a simple term we repeat the simulation with random constant torque of the ankle roll joint. The CoM in the frontal plane trajectory is:

$$\begin{aligned} E_{d-f}(r_{Cx}) \;=\; & -11926 r_{Cx}^6 - 2087.1 r_{Cx}^5 + 657.95 r_{Cx}^4 \\ & +151.42 r_{Cx}^3 + 46.79 r_{Cx}^2 \\ & -0.5337 r_{Cx} - 0.0024. \qquad (28) \end{aligned}$$

Consequently the second control method for the ankle roll joint is:

$$\boldsymbol{\tau}_{emp} = \begin{bmatrix} k\{E_{d-f}(r_{Cx}) - E_f\} \\ 0 \\ 0 \end{bmatrix}, \qquad (29)$$

where k is a constant positive feedback gain.

IV. NUMERICAL SIMULATION

The control torque for the conservation of the pitch motion limit cycle is:

$$\boldsymbol{\tau}_{lc} = \boldsymbol{\tau}_{dcp} + \boldsymbol{\tau}_g + \boldsymbol{\tau}_{ef3} + \boldsymbol{\tau}_{lock}. \qquad (30)$$

Besides, we consider two kinds of control for the roll motion. Consequently we deal with two kinds of simulations with control torques $\boldsymbol{\tau} = \boldsymbol{\tau}_{lc} + \boldsymbol{\tau}_{spl}$ and $\boldsymbol{\tau} = \boldsymbol{\tau}_{lc} + \boldsymbol{\tau}_{emp}$ respectively where the constant spline coefficients are $a_0 = 0$ $a_1 = 0.51$ $a_2 = 0$ $a_3 = -0.99$ $a_4 = -0.96$ $a_5 = 1.36$ and $k = 3000$ Nm/rad. Figure 6 shows the simulation result of Limit Cycle Walking with the control torque $\boldsymbol{\tau} = \boldsymbol{\tau}_{lc} + \boldsymbol{\tau}_{spl}$. Figure 6(a) shows the phase portrait. The robot walks periodically. However we are not satisfied with the trajectory of q_1 vs $\dot{q}_1$ in this phase portrait because the shape of the trajectory is awkward. Therefore we conclude that roll motion is quite unnatural motion. Figure 6(b) shows the joint torque. Figure 7 shows the simulation result of Limit Cycle Walking with the control torque $\boldsymbol{\tau} = \boldsymbol{\tau}_{lc} + \boldsymbol{\tau}_{emp}$. Figure 7(a) shows the phase portrait. The robot walks periodically. We compare the trajectory of q_1 vs $\dot{q}_1$ in this phase portrait with the respective trajectory in Fig. 6(a).

V. CONCLUSIONS AND FUTURE WORKS

A. Conclusions

In this paper we designed a biped controller based on Limit Cycle Walking. Concretely we adopted energy feedback control for pitch motion. Hence, pitch motion became robust and the limit cycle was ensured. Consequently we regarded the coupling from the roll motion at the collision as an external disturbance and resolved the problem. Roll motion was controlled via tracking control with a reference trajectory which has non–zero velocity at the initial and the final states. We choose two types of reference trajectories (Eqs. (26) and (28)). The trajectory in Fig. 7(a) has a neat shape. This suggests that the roll motion is optimized by our repeated empirical method. Consequently the roll motion control with the empirical reference trajectory is superior to that of the analysis of the equation of collision. We can conclude that the method of analysis of the equation of collision was successful. However the method of generation of the trajectory that satisfies the analysis, was unsuitable.

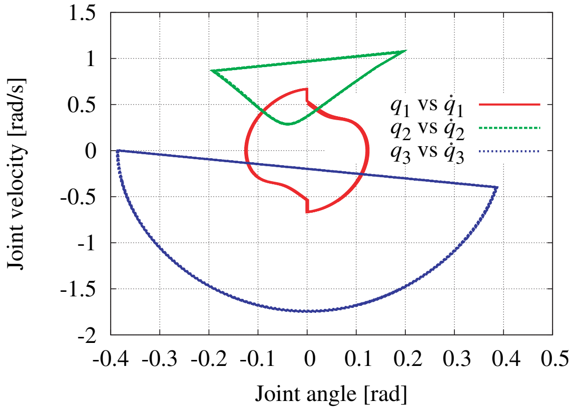

(a) Phase portrait.

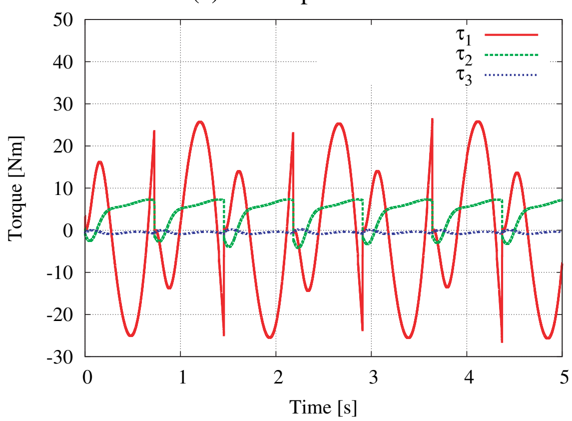

(b) Joint torque.

Fig. 6. Simulation results of the simplest 3D Limit Cycle Walking with control torque $\boldsymbol{\tau} = \boldsymbol{\tau}_{lc} + \boldsymbol{\tau}_{spl}$.

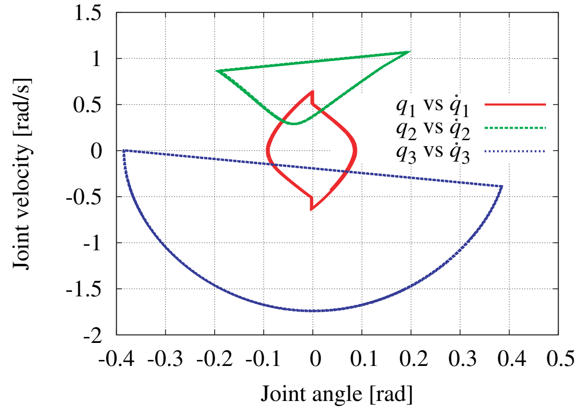

(a) Phase portrait.

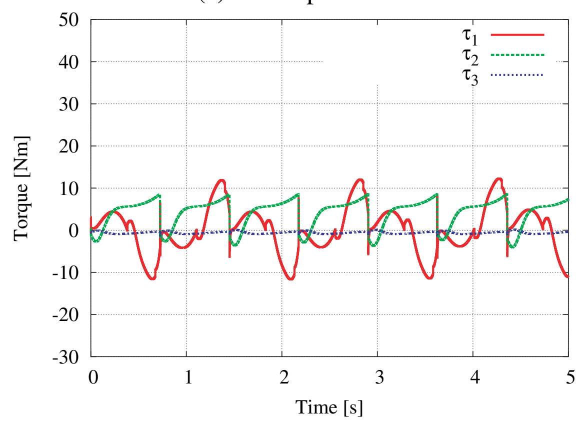

(b) Joint torque.

Fig. 7. Simulation results of the simplest 3D Limit Cycle Walking with control torque $\boldsymbol{\tau} = \boldsymbol{\tau}_{lc} + \boldsymbol{\tau}_{emp}$.

Consequently we should not use a spline function for generation of the trajectory. Hence, we have to deal with a new problem: how to generate a reference trajectory for the ankle roll joint?

B. Future works

Our purpose is to apply the control based on Limit Cycle Walking to humanoid robots. We summarize the problems and assignments of 3D Limit Cycle Walking as follows. It is needed:

- to optimize the reference trajectory of the ankle roll joint.
- to consider pitch motion stabilization because we don't think that energy feedback control is the best solution.

REFERENCES

[1] S. Kajita and T. Sugihara, "Humanoid Robots in the Future," *J. RSJ*, vol. 26, no. 7, pp. 761–762, 2008.

[2] M. Vukobratovich, B. Borovac, D. Surla and D. Stokic, "Biped Locomotion, Stability, Control and Application," *Springer Verlag*, 1990.

[3] S. Kajita, "Biped Walking," in *Humanoid Robot*, Ed. Tokyo: Ohmsha, 2005, pp. 103–161.

[4] T. Sugihara and Y. Nakamura, "High Mobility Control of Humanoid Robots Based on an Analogy of ZMP–COG Model and Carted Inverted Pendulum Model," *J. RSJ*, vol. 24, no. 1, pp. 74–86, 2006.

[5] D.N. Nenchev, Y. Tsumaki and A. Sekiguchi, "Motion Feedback Control at a Singular Configuration," *The Society of Instrument and Control Engineers SystemIntegration Division*, Tokyo, Dec, 2003, pp. 508–509.

[6] Y. Ogura, T. Kataoka, K. Shimomura, H. Lim, A. Takanishi, "A Novel Method of Biped Walking Pattern Generation with Predetermined Knee Joint Motion," *in Proc. 2004 IEEE/RSJ Int. Conf. on Inteligent Robotics and Systems*, 2004, pp. 2381–2386.

[7] R. Kurazume, S. Tanaka, M. Yamashita, T. Hasegawa, "Straight Legged Walking of a Biped Robot," *in Proc. 2005 IEEE/RSJ Int. Conf. on Inteligent Robotics and Systems*, 2005, pp. 3095–3101.

[8] K. Takahashi, M. Noda, D. N. Nenchev, Y. Tsumaki and A. Sekiguchi, "Static Walk of a Humanoid Robot Based on the Singularity-Consistent Method", *in Proc. 2006 IEEE/RSJ Int. Conf. on Inteligent Robotics and Systems*, 2006, pp. 5484–5489.

[9] T. McGeer, "Passive Dynamic Walking," *The Int. J. of Robotics Research* , vol.9, no.2, pp.62-82, 1990.

[10] T. McGeer, "Passive Dynamic Walking Catalogue," *in Proc. Int. Sysmp. Exper. Robot.*, pp. 465–490, 1991.

[11] A. Kuo, "Stabilization of Lateral Motion in Passive Dynamic Walking," *The Int. J. of Robotics Research*, vol. 18, no. 9, pp. 917–930, 1999.

[12] M. Wisse, A. L. Schwab, R. Q. vd. Linde, "A 3D Passive Dynamic Biped with Yaw and Roll Compensation," *Robotica*, vol. 19, pp. 275–284, 2001

[13] D.G.E. Hobbelen and M. Wisse, "Limit Cycle Walking," in *Humanoid Robots: Human-like Machine*, Ed. Austria: I-Tech, 2007, pp. 277–294.

[14] F. Asano and Zhi–Wei Luo, and M. Yamakita, "Biped Gait Generation and Control Based on a Unified Property of Passive Dynamic Walking," *IEEE Trans. Robotics*, vol. 21, no. 4, pp. 754–762, Aug, 2005.